

**Viscoplasticity and large-scale chain relaxation in glassy-polymeric strain hardening**

Robert S. Hoy\* and Corey S. O'Hern

*Department of Mechanical Engineering and Materials Science, Yale University, New Haven, Connecticut 06520-8286, USA  
and Department of Physics, Yale University, New Haven, Connecticut 06520-8120, USA*

(Received 2 April 2010; revised manuscript received 6 August 2010; published 13 October 2010)

A simple theory for glassy-polymeric mechanical response that accounts for large-scale chain relaxation is presented. It captures the crossover from perfect-plastic response to Gaussian strain hardening as the degree of polymerization  $N$  increases, without invoking entanglements. By relating hardening to interactions on the scale of monomers and chain segments, we correctly predict its magnitude. Strain-activated relaxation arising from the need to maintain constant chain contour length reduces the characteristic relaxation time by a factor  $\sim \dot{\epsilon}N$  during active deformation at strain rate  $\dot{\epsilon}$ . This prediction is consistent with results from recent experiments and simulations, and we suggest how it may be further tested experimentally.

DOI: [10.1103/PhysRevE.82.041803](https://doi.org/10.1103/PhysRevE.82.041803)

PACS number(s): 61.41.+e, 62.20.F-, 81.40.Lm, 83.10.Rs

**I. INTRODUCTION**

Developing a microscopic analytic theory of glassy-polymeric mechanical response has been a long-standing challenge. Plasticity in amorphous materials is almost always *viscoplasticity*, i.e., plasticity with rate dependence. Many recent studies have focused on plasticity in metallic or colloidal glasses. Relative to these systems, polymer glasses possess a wider range of characteristic length and time scales because of the connectivity, uncrossability, and random-walk-like structure of the constituent chains. These alter the mechanical properties significantly [1]; for example, a uniquely polymeric feature of plastic response is massive strain hardening beyond yield.

The relationships between polymeric relaxation times on different spatial scales are fairly well understood for melts [2] but much less so for glasses. Recent experiments [3–5], simulations [5–7], and theories [8,9] have all shown that local (segment-level) relaxation times in polymer glasses decrease dramatically under active deformation (especially at yield) and increase when deformation is ceased. Analysis of these phenomena has focused on stress-assisted thermal activation of the local relaxation processes, but it is likely that other structural relaxation processes at larger scales or of different (e.g., strain-activated) character are also important in determining the mechanical response. Improved understanding of the concomitant scale-dependent relaxation is necessary to better understand polymeric plasticity and material failure. However, theoretical prediction of large-scale relaxation in deformed polymer glasses is still in its infancy; most treatments evaluate mechanical response “neglecting the effect of the ongoing structural relaxation during the experiment” [10].

In this paper, we develop a theory that treats large-scale relaxation of uncross-linked chains during active deformation. Stress in the postyield regime is assumed to arise from local plastic rearrangements similar to those which control plastic flow; as strain increases, these increase in rate with the volume over which they are correlated. Polymeric strain

hardening is thus cast as plastic flow in a medium where the effective flow stress increases with large-scale chain orientation. Relaxation of chain orientation is treated here as inherently strain-activated and *coherent*, i.e., cooperative along the chain backbone.

Our theory predicts a continuous crossover from perfect plasticity to “Gaussian” (Neohookean) [11] strain hardening as the degree of polymerization  $N$  increases. The latter form is predicted when chains deform affinely on large scales and corresponds to the limit where the system is deformed faster than chains can relax. A key difference from most previous theories is that instead of invoking entanglements, we relate the time scale  $\tau$  for large-scale chain relaxation to the segmental relaxation time  $\tau_\alpha$ . This is consistent with (i) the picture that stress arises predominantly from local plasticity [12], (ii) recent dielectric spectroscopy experiments indicating connections between relaxations on small and large scales [13], and (iii) recent NMR experiments [14] that have found the effective “constraint” density for deformed glasses is much larger than the entanglement density measured in the melt. By relating strain hardening to interactions on the scale of monomers and segments, we make a prediction of its magnitude that is consistent with the underlying glassy physics. We test our predictions using coarse-grained molecular-dynamics simulations, and in all cases find (at least) semi-quantitative agreement.

The rest of this paper is organized as follows. In Sec. II we motivate and develop the theory for mechanical response, make predictions that illustrate the effect of coherent relaxation in constant-strain-rate deformation and constant-strain relaxation experiments, and test these using simulations. In Sec. III, we summarize our results, place our work in the context of recent theories and experiments, discuss how the model could be more quantitatively tested experimentally, and conclude.

**II. THEORY AND SIMULATIONS****A. Background**

Consider a bulk polymer sample deformed to a macroscopic stretch  $\bar{\lambda}$ . Classical rubber elasticity relates the de-

\*robert.hoy@yale.edu

TABLE I. Functional forms for strain hardening assuming affine constant-volume deformation by a stretch  $\lambda$ .

Deformation mode	$\bar{\lambda}$	$g(\lambda)$	$\bar{g}(\lambda)$
Uniaxial	$\lambda_x = \lambda_y = \lambda_z^{-1/2}$	$\lambda^2 - 1/\lambda$	$1/3(\lambda^2 + 2/\lambda)$
Plane strain	$\lambda_x = \lambda_z^{-1}, \lambda_y = 1$	$\lambda^2 - \frac{1}{\lambda^2}$	$1/3(\lambda^2 + 1 + 1/\lambda^2)$

crease in entropy density to  $\bar{g}(\bar{\lambda}) = \frac{1}{3}(\lambda_x^2 + \lambda_y^2 + \lambda_z^2)$  [15,16]. Phenomenological ‘‘Neohookean’’ theories assume a strain energy density of the same form. Both approaches give an associated (true) stress  $\sigma \propto \partial \bar{g}(\bar{\lambda}) / \partial \ln(\bar{\lambda}) \equiv g(\bar{\lambda})$ . All results in this paper are presented in terms of true stresses and strains. Stress-strain curves in well-entangled polymer glasses are often fit [11] by  $\sigma(\bar{\lambda}) = \sigma_0 + G_R g(\bar{\lambda})$ , where  $\sigma_0$  is comparable to the plastic flow stress  $\sigma_{flow}$  and  $G_R$  is the strain hardening modulus. Because of this, strain hardening has traditionally been associated [17] with the change in entropy of an affinely deformed entangled network, with  $G_R$  assumed to be proportional to the entanglement density  $\rho_e$ . Forms for  $\bar{g}(\lambda)$  and  $g(\lambda)$  for the most commonly imposed deformation modes are given in Table I; Fig. 1(a) depicts the ‘‘uniaxial’’ case.

There are, however, many problems with the entropic description [18–20]. One is that chains in uncross-linked glasses will not, in general, deform affinely at large scales comparable to the radius of gyration. Rather, they will pos-

sess a chain-level stretch  $\bar{\lambda}_{eff}$  [Fig. 1(a)] which describes the deformation of chains on large scales; for example, its  $zz$  component is  $\langle R_z/R_z^0 \rangle$ , where  $R_z$  is the  $z$  component of the rms end-to-end distance  $R_c$  and  $R_z^0$  is its value in the undeformed glass. The deformation of well-entangled chains is consistent with an affine deformation,  $\bar{\lambda}_{eff} = \bar{\lambda}$ , while for unentangled systems the deformation is subaffine [21]. Hereon, we drop tensor notation, e.g.,  $\bar{\lambda} \rightarrow \lambda$ , but all quantities remain tensorial.

A key insight is that the evolution of stress in polymer glasses is controlled by the stretch  $\lambda_{eff}$  of chains on scales comparable to their radius of gyration and only indirectly by  $\lambda$ . Well below the glass transition temperature  $T_g$ , stress is well described [22,23] by

$$\sigma(\bar{\lambda}) = \sigma_0 + G_R^0 g(\lambda_{eff}), \quad (1)$$

where  $G_R^0$  is the value of  $G_R$  in the long-chain limit [24].

Equation (1) shows that predicting  $\lambda_{eff}$  is a critical component of the correct theory for the mechanics of uncross-linked polymer glasses. However, to our knowledge, no simple microscopic theory that predicts the functional form of  $\lambda_{eff}$  in glasses has been published. Most viscoelastic and viscoplastic constitutive models that describe strain hardening (e.g., Refs. [25,26]) decompose  $\lambda$  into rubber-elastic and plastic parts or use other internal state variables but do not explicitly account for  $\lambda \neq \lambda_{eff}$  or the  $N$  dependence of non-affine relaxation [27–32]. In this paper we do so;  $\lambda_{eff}$  is treated as a mesoscopic (chain-level) internal state variable [27,28].

## B. Maxwell-like model for $\lambda_{eff}$

We now develop a predictive theory for  $\lambda_{eff}$ . The problem is most naturally formulated in terms of true strains  $\epsilon_{eff} = \ln(\lambda_{eff})$  and  $\epsilon = \ln(\lambda)$ . We postulate a simple Maxwell-like model for the relaxation of  $\epsilon_{eff}$ . The governing equation for the model shown in Fig. 1(b) is

$$\dot{\epsilon}_{eff} = \dot{\epsilon} - \epsilon_{eff} / \tau. \quad (2)$$

Equation (2) is a standard ‘‘fading memory’’ form implying chains ‘‘forget’’ their large-scale orientation at a rate  $\tau^{-1}$ . In other words,  $\tau$  is the time scale over which  $\epsilon_{eff}$  will relax toward its ‘‘equilibrium’’ value  $\epsilon_{eff} = 0$  (we assume that chains are not cross-linked).

In this formulation  $\epsilon_{eff}$  corresponds to the strain in the ‘‘spring’’ in Fig. 1(b). However, the stress we will associate with increasing  $|\epsilon_{eff}|$  is *viscoelastoplastic*. Here,  $\epsilon_{eff}$  is an (in principle) *microreversible* strain corresponding to chain orientation; it is not an elastic strain in the macroscopic sense of shape recoverability of a bulk sample [33].  $\epsilon_{pl} \equiv \epsilon - \epsilon_{eff}$  corresponds to the ‘‘dashpot’’ strain used in many constitutive models; it is plastic in the sense of being both microirreversible and macroirreversible.

Maxwell-like models have been used to describe polymer viscoelasticity for more than half a century, and complicated ladder models were developed (e.g., Ref. [34]) because of the inadequacy of earlier single rate models. However, we will provide evidence below that the correct choice of meso-

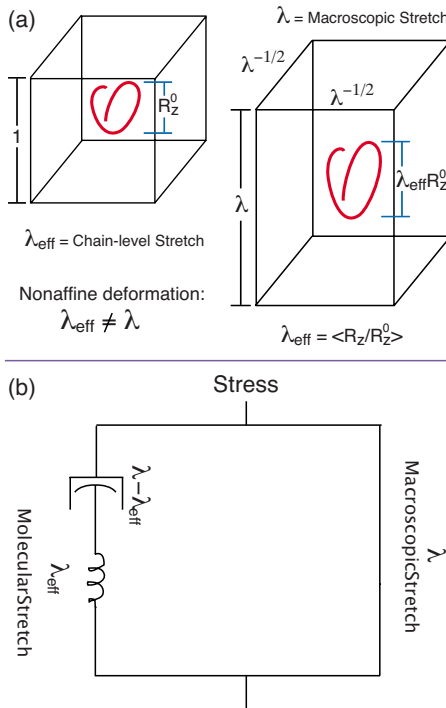


FIG. 1. (Color online) Schematic of our model. (a)  $\lambda$  is the macroscopic stretch (observed on the scale of the experimental sample if deformation is homogeneous), while  $\lambda_{eff}$  is the large-scale chain stretch. Constant-volume uniaxial deformation is depicted. (b) The spring-dashpot model for the nonaffine chain response is described in Eq. (2).

variable (i.e.,  $\lambda_{eff}$  or  $\epsilon_{eff}$ ) restores the applicability of a single (albeit  $N$ -dependent) relaxation-time model, at least for monodisperse systems.

### C. Coherent strain-activated relaxation

The next step in constructing a useful microscopic theory is prediction of  $\tau$ . If one supposes that chains under active deformation at strain rate  $\dot{\epsilon}$  relax *coherently* and that the relaxation is strain activated,  $\tau$  is reduced by a factor of  $N\dot{\epsilon}$  relative to its quiescent value.

We assume that relaxation on large scales is coupled to segmental relaxation. For an *a priori* unspecified relaxation dynamics in the quiescent state,

$$\tau \sim N^\gamma \tau_\alpha \quad (\text{incoherent}), \quad (3)$$

where  $\tau_\alpha$  is the ‘‘alpha’’ or segmental relaxation time and  $\gamma$  is unspecified and may be  $N$  dependent.

Gaussian polymers have chain statistics defined by  $R_c^2 \equiv R_s^2 N$ , where  $R_s^2$  is the squared statistical segment length. Mathematically, this gives the identity

$$\partial R_c^2 / \partial t = N \partial R_s^2 / \partial t. \quad (4)$$

While Eq. (4) surely oversimplifies the physics of glasses (e.g., it does not hold in quiescent systems because  $R_c^2$  is stationary), nonetheless it suggests an associated relaxation rate under active deformation that is  $N$  times larger (or a time  $N$  times smaller) than the value in the quiescent state,

$$\tau \sim N^{\gamma-1} \tau_\alpha \quad (\text{coherent}). \quad (5)$$

We postulate that Eq. (4) becomes valid in actively deformed glasses; segmental rearrangements become coherent because rearrangements that restore  $R_c^2$  toward its initial value dominate over those which do not. In practice, coherent relaxation is forced by the stiffness of the covalent backbone bonds, which have (nearly) constant length  $l_0$  and so maintain (nearly) constant chain contour length  $L = (N-1)l_0$ .

Recent work assists in hypothesizing a more specific relaxation dynamics for actively deformed systems. Hoy and Robbins [23] showed that chains in not-too-densely [35] entangled model polymer glasses well below  $T_g$  orient independently of one another during active deformation. The behavior observed was that of individual chains coupled to a ‘‘mean-field’’ glassy medium. If relaxations on chain and segmental scales are *tightly* coupled and chains relax independently of one another,  $\gamma=2$  is predicted [2]. Then,

$$\tau \sim N^2 \tau_\alpha \quad (\text{incoherent}),$$

$$\tau \sim N \tau_\alpha \quad (\text{coherent}). \quad (6)$$

Within the framework of Eqs. (3), (5), and (6), when relaxation is strain activated, both  $\tau_\alpha$  [8] and  $\tau$  will be reduced by a factor  $\sim \dot{\epsilon}$ , so the overall reduction in  $\tau$  during active deformation scales as  $N\dot{\epsilon}$ . Note that the scaling analysis presented above does not account for additional changes in  $\tau_\alpha$  arising from other causes, e.g., increased mobility associated with yield. Also note that the above arguments assume  $\epsilon_{eff}$  and  $\dot{\epsilon}$  have the same sign. If deformation is reversed, e.g., in

a Bauschinger-effect experiment [36,37], and the sign of  $\dot{\epsilon}$  is opposite that of  $\epsilon_{eff}$ , active deformation may not produce coherent relaxation.

### D. Bead-spring simulations

Some of the arguments made in Secs. II B and II C were heuristic, and several assumptions were made, so it is important to compare the theoretical predictions with results from simulations. For example, observations of sharp changes in segmental relaxation times with strain and significant dynamical heterogeneity [4,5,7] during deformation are seemingly at odds with our postulated single constant relaxation time  $\tau$ . Further, entangled chains may not be able to relax coherently if the entanglements concentrate stress, so the reduction of  $\tau$  in actively deformed entangled systems may be weaker than predicted above.

The basic ideas presented above can be tested using molecular-dynamics simulations of the Kremer-Grest bead-spring model [38]. All MD simulations were performed using LAMMPS [39]. Polymer chains are formed from  $N$  monomers of mass  $m$ . All monomers interact via the truncated and shifted Lennard-Jones potential  $U_{LJ} = 4u_0\{(a/r)^{12} - (a/r)^6 - [(a/r_c)^{12} - (a/r_c)^6]\}$ . Here,  $r_c = 1.5a$ . Covalently bonded monomers additionally interact via the finitely extensible nonlinear elastic (FENE) potential  $U_{FENE} = -(kR_0^2/2)\ln[1 - (r/R_0)^2]$ ; the canonical [38] values  $k = 30u_0/a^2$  and  $R_0 = 1.5a$  are employed. All quantities are expressed in terms of the intermonomer binding energy  $u_0$ , monomer diameter  $a$ , and characteristic time  $\tau_{LJ} = \sqrt{ma^2/u_0}$ . The equilibrium covalent bond length is  $l_0 = 0.96a$  and the Kuhn length in the melt state is  $l_K = 1.8a$ .

All systems have  $N_{ch}$  chains, with  $N_{ch}N \approx 2.5 \times 10^5$ . Periodic boundary conditions are applied along all three directions of the simulation cell, which has periods  $L_x, L_y, L_z$  along the  $x, y, z$  directions. Melts are equilibrated [41] and rapidly quenched ( $k_B \dot{T} = -0.002u_0/\tau_{LJ}$ ) into glasses at  $T = 0.2u_0/k_B \approx 0.6T_g$ . Uniaxial-stress compressive deformations are then imposed. [22] A constant true strain rate  $\dot{\epsilon} = \dot{L}_z/L_z = -10^{-5}/\tau_{LJ}$  is applied, with  $\lambda = L_z/L_z^0$ . A Langevin thermostat with damping time  $10\tau_{LJ}$  is used to maintain  $T$ , and a Nose-Hoover barostat with damping time  $100\tau_{LJ}$  is used to maintain zero pressure along the transverse directions. The values of  $|\dot{\epsilon}|$  and  $T$  employed here lie within ranges shown [42,43] to reproduce many experimental trends [1], such as logarithmic dependence of  $\sigma$  on  $\dot{\epsilon}$  and linear scaling of the hardening modulus with the flow stress.

### E. Chain conformations under deformation and constant-strain relaxation

Constant-strain-rate deformation and constant-strain relaxation are two of the most commonly performed mechanical experiments. In a constant-strain rate experiment, assuming  $\tau$  is independent of  $\epsilon$ , i.e., assuming polymer glasses are *linearly* viscoplastic, the solution to Eq. (2) is [44]

$$\epsilon_{eff}(\epsilon) = \dot{\epsilon}\tau[1 - \exp(-\epsilon/\dot{\epsilon}\tau)] \equiv \dot{\epsilon}\tau[1 - \exp(-t/\tau)]. \quad (7)$$

If a system is deformed to a strain  $\epsilon^0$  and effective strain  $\epsilon_{eff}^0$  and then deformation is ceased, Eq. (2) has the solution

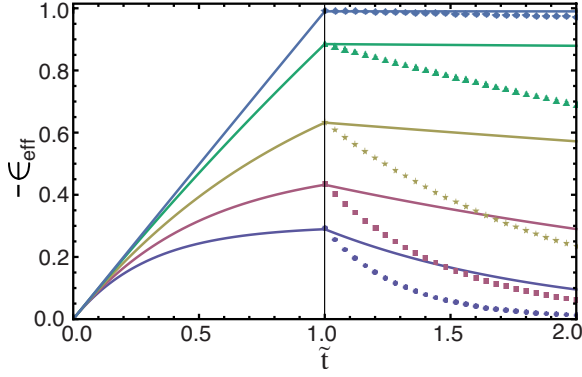


FIG. 2. (Color online) Compressive deformation followed by relaxation at constant strain. Curves from top to bottom are for  $N=500$ ,  $N=40$ ,  $N=10$ ,  $N=5$ , and  $N=3$ .  $\tilde{t}=|\dot{\epsilon}|t$  is time scaled by the strain rate applied for  $0 \leq \tilde{t} \leq 1$ . For  $\tilde{t} < 1$  curves show predictions of Eq. (7), while for  $\tilde{t} > 1$  curves and symbols show predictions of Eq. (8). Solid curves assume  $\tau \propto N^{\gamma-1}$  during deformation and  $N^\gamma$  at constant strain, while symbols assume  $\tau \propto N^{\gamma-1}$  at all  $\tilde{t}$ . Here,  $\gamma=2$ .

$$\epsilon_{eff} = \epsilon_{eff}^0 \exp(-t/\tau). \quad (8)$$

In this case, our model predicts slowdown in relaxation upon cessation of deformation; the  $\tau$  in Eq. (8) is  $N\dot{\epsilon}^{-1}$  times larger than the  $\tau$  in Eq. (7).

Figure 2 shows theoretical predictions of Eqs. (7) and (8) for evolution of  $\epsilon_{eff}(t)$  in systems compressively strained to  $\epsilon=-1.0$  at constant rate (for  $0 < t < \dot{\epsilon}^{-1}$ ) and then allowed to relax at constant strain. Results are plotted against  $\tilde{t}=\dot{\epsilon}t$ , where  $\dot{\epsilon}$  is the strain rate applied during compression. For the purpose of contrast, the symbols show predictions assuming that relaxation remains coherent (i.e.,  $\tau$  increases by only a factor  $\dot{\epsilon}^{-1}$ ) after deformation is ceased.  $N=500$  chains orient nearly affinely during strain,  $\epsilon_{eff} \approx \dot{\epsilon}t$ , while short chains orient much less. The solid lines are far more consistent with both experiments [3–5] and simulations [6,7], which show relaxation slows dramatically upon cessation of active deformation.

Figure 3 shows simulation data for  $\epsilon_{eff}(t)$  under the same procedure of compression followed by constant-strain relaxation. Solid lines for  $\tilde{t} \leq 1$  are fits to Eq. (7). Values for  $\tau$  from these fits are given in Table II. The data are quantitatively consistent with  $\tau \propto N^{\gamma-1}$  and  $\gamma=2$ . In particular, values for  $\tau/(N-1)$  are nearly constant. For this model, careful topological analyses and rheological simulations have shown [45,46] that the entanglement length is  $N_e \approx 85$ , so the trend spans the range from unentangled to well-entangled chains. The effect of entanglements is more consistent with an increase in the prefactor of  $\tau/(N-1)$  than a change in  $\gamma$ .

As shown in Table II, the agreement of  $\tau$  with the prediction  $\tau_\alpha \approx 0.1\dot{\epsilon}^{-1}$  under active deformation [8], where we identify  $\tau_\alpha = \tau/(N-1)^{\gamma-1}$ , is quantitative. The data in Fig. 3 are consistent with our assumption that  $\tau$  remains constant during deformation; only small deviations from the fits to Eq. (7) are apparent on the scale shown. Given the large variation in stress as strain increases (see Sec. II G), it is remarkable that a single relaxation rate theory fits  $\epsilon_{eff}$  so well. However, this is consistent with the enhancement of

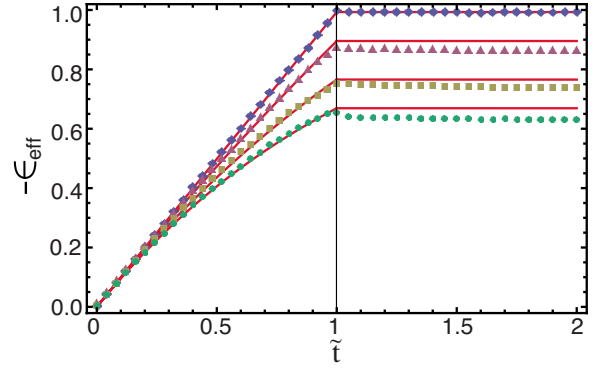


FIG. 3. (Color online)  $\epsilon_{eff}$  vs  $\tilde{t}$  for uniaxial compression followed by constant-strain relaxation; comparison of theory and simulation results. Symbols from top to bottom are bead-spring simulation results for  $N=500$ , 36, 18, and 12. For  $\tilde{t} \leq 1$ , lines are fits to Eq. (7); the fit values of  $\tau$  are given in Table II. For  $\tilde{t} \geq 1$  the lines are given in Eq. (8); no further fitting is employed, and the values of  $\tau$  from Table II are multiplied by  $N\dot{\epsilon}^{-1}$ , consistent with the transition from coherent to incoherent relaxation assumed to occur upon cessation of deformation.

dynamical homogeneity and narrowing of the relaxation spectrum under flow observed in similar models in Refs. [7,47]. In developing our theory for the mechanical response, we will assume for simplicity that  $\tau$  is indeed independent of  $\epsilon$ .

After cessation of deformation, simulation results in Fig. 3 suggest that Eqs. (2) and (8) give a qualitatively valid description of large-scale chain relaxation at constant strain. The small initial decreases in  $|\epsilon_{eff}|$  at times  $(\tilde{t}=1+\delta, \delta \ll 1)$  are larger than the theoretical predictions of Eq. (8) for small  $N$ . This may be attributable to chain end or segmental-relaxation effects not included in our model. At larger  $\tilde{t}$ , however, it is clear that the increase in  $\tau$  upon cessation of deformation is qualitatively captured.

#### F. Microscopic theory for viscoplastic stress

Here, we will derive a theory of Neoohookean viscoplasticity for the  $N$ -dependent stress-strain response. The work to

TABLE II. Values of  $\tau$  obtained by fitting  $\epsilon_{eff}(t)$  to Eq. (7) (with  $\gamma=2$ ) as a function of chain length  $N$  for flexible bead-spring chains. For these systems,  $N_e \approx 85$  [45]. Statistical uncertainties on  $\tau$  are estimated at 5%. The factor of  $N-1$  in the rightmost column arises because in a discrete-bead model, relaxation is associated with the number of covalent bonds rather than monomers. Note  $\dot{\epsilon} = 10^{-5}/\tau_{LJ}$  so  $\dot{\epsilon}\tau$  is on the order of unity for chains with  $N \sim 10$ .

$N$	$\tau/\tau_{LJ}$	$\tau/[(N-1)\tau_{LJ}]$
12	$1.15 \times 10^5$	$1.05 \times 10^4$
18	$1.78 \times 10^5$	$1.05 \times 10^4$
36	$4.49 \times 10^5$	$1.09 \times 10^4$
71	$7.19 \times 10^5$	$1.03 \times 10^4$
107	$1.12 \times 10^6$	$1.05 \times 10^4$
250	$2.76 \times 10^6$	$1.11 \times 10^4$
500	$7.14 \times 10^6$	$1.43 \times 10^4$

deform the system is broken into two components corresponding to an isotropic resistance to flow and an anisotropic resistance to chain orientation. This general approach has been employed many times before, e.g., in Refs. [17,48]. Here we present a microscopic picture that quantitatively associates the Gaussian or Neohookean strain hardening with the energy dissipated in local segmental hops and quantitatively associates the smaller hardening observed for shorter chains to strain-activated relaxation of large-scale chain orientation (i.e.,  $\lambda \neq \lambda_{eff}$ ).

From the second law of thermodynamics, the work  $W$  required to deform a polymer glass is  $W(\epsilon) = \Delta E(\epsilon) + \Delta Q(\epsilon)$ , where  $E$  is the internal energy and  $Q$  is the portion of work converted into heat, including both dissipative and entropic terms. Without loss of generality, this can be rewritten as  $W(\epsilon) = W_1(\epsilon) + W_2(\epsilon)$ , where  $W_2$  is the viscoplastic component of the work.  $W_1$  captures “everything else,” such as elastic terms preyield and (in principle, though they are not treated in this paper) other effects such as softening, anelastic energetic stresses, and entropic stresses. In experiments, ductile deformation of glassy polymers occurs at nearly constant volume [1]; thus, we assume constant-volume deformation and treat  $W_1$  and  $W_2$  as intensive quantities.

Both rubber elasticity and Neohookean elasticity associate strain hardening with  $W_1$ . However, experiments and simulations [19,22] have shown that  $W_2$  is the dominant term for strains ranging from the beginning of the plastic flow regime to the onset of dramatic “Langevin” [17] hardening. The latter occurs at very high strains for most synthetic polymers [11] and has been associated with the increase in energy arising from chain stretching between entanglements [22,49]. Simulations have provided strong evidence that in this regime,  $W_2$  is closely connected with the same local interchain plastic events that control the flow stress [22]. These events have a characteristic energy density  $\sim u_0/a^3$ , where  $u_0$  is the energy scale of secondary (i.e., noncovalent) interactions [50]. Here, we treat the regime where  $W_2$  dominates and neglect  $W_1$ , i.e., we make the approximation  $W = W_2$ .

$W$  may be further broken down into “segmental” and “polymeric” terms:  $W = W^s + W^p$ , where  $W^s$  accounts for the plastic flow stress in the absence of hardening and  $W^p$  accounts for the viscoplastic component of strain hardening. Since this paper focuses on strains well beyond yield, for convenience we choose a standard viscous-yield term

$$W^s = \frac{u_0}{a^3} [\epsilon + \epsilon_y \exp(-\epsilon/\epsilon_y)], \quad (9)$$

where  $\epsilon_y$  is the yield strain.

The stress is given by  $\sigma = \partial W / \partial \epsilon$ . It can similarly be written as a sum of segmental and polymeric contributions,

$$\sigma = \sigma^s + \sigma^p = \partial W^s / \partial \epsilon + \partial W^p / \partial \epsilon. \quad (10)$$

Reference [22] showed that  $\sigma \propto R_p$ , where  $R_p$  is the rate (per unit strain) of plastic events identified by local rearrangements. The natural correlation length scale for the local plastic rearrangements, since according to the above arguments they are coherent, is  $R_c$ , and the associated volume is  $V = R_c^3/6^{3/2}$ . Here, factors of  $\sqrt{6}$  arise from the standard relation

for the radius of gyration  $R_g$  of Gaussian polymers,  $R_g = R_c/\sqrt{6}$ .

We will now associate polymeric strain hardening with  $W^p$  and replace  $\lambda$  by  $\lambda_{eff}$  in order to calculate an  $N$  dependent  $\sigma^p$ . We postulate that  $W^p$  is controlled by the increase in  $V$ ; in other words, strain hardening occurs because the volume  $V$  controlling  $W^p$  increases faster than it can relax [51]. Studies of bidisperse mixtures have provided strong evidence that the evolution of  $\lambda_{eff}$  (and hence strain hardening) can be understood in terms of single chains interacting with a glassy mean field [23], so it is natural to assume the plastic events are “unary” (in the sense that  $\geq 2$ -chain effects are unimportant).  $W^p$  will then scale linearly with  $\rho_{cr}$ , where

$$\rho_{cr} = \sqrt{6} \rho l_0 / (NR_c) \quad (11)$$

is the density of coherently relaxing contours and  $\rho$  is monomer number density. Then, incrementally,

$$\Delta W^p \simeq (u_0/a^3) \Delta(\rho_{cr} V) = (u_0/a^3) N^{-1} \rho l_0 \Delta(R_c^2)/6. \quad (12)$$

Recall  $R_c^2 = 3l_0 l_K N \bar{g}(\lambda_{eff})$ , where  $l_K$  is (here) the equilibrium Kuhn length in the undeformed glass. For a deformation increment  $\Delta\bar{\lambda}$ ,

$$\Delta(R_c^2) = 2l_0 l_K N \Delta[\bar{g}(\lambda)|_{\lambda_{eff}}], \quad (13)$$

where  $g(\epsilon) = (3/2) \partial \bar{g} / \partial \epsilon$ . The term in parentheses indicates that the difference is evaluated at  $\lambda = \lambda_{eff}$ .

Combining Eqs. (12) and (13) gives

$$\Delta W^p = (u_0/a^3) \rho l_0^2 l_K \Delta[\bar{g}(\lambda_{eff})]/2. \quad (14)$$

This result combined with Eq. (9) gives a prediction for the stress,

$$\sigma(\epsilon_{eff}) = \frac{u_0}{a^3} [1 - \exp(-\epsilon/\epsilon_y) + \rho l_0^2 l_K |g(\epsilon_{eff})|/2], \quad (15)$$

The absolute value  $|g(\epsilon_{eff})|$  appears because we have so far treated  $\sigma$  as positive.

Equation (15) has several interesting features, which we now relate to previous models. First, it predicts that  $\sigma^p$  (at fixed strain) increases with increasing  $l_K$ . This is consistent with the well-established result that straighter chains are harder to plastically deform [1,11]. However, the power of  $l_K$  on which  $\sigma^p$  depends is sensitive to our theoretical assumptions, specifically the definition of  $\rho_{cr}$  [Eq. (11)]. Other definitions can produce  $G_R \propto l_K^{3/2}$  or  $l_K^3$ , but choosing which one is “best” [52] requires greater knowledge of the variation in local plasticity (at a microscopic level) with  $l_K/l_0$  than is currently available. We test Eq. (15) using molecular dynamics (MD) simulations in Sec. II G. While only one value of  $l_K/a$  is considered here, it is large enough (1.8) that viscoplastic contributions to  $\sigma$  scaling as  $l_K^3$  would be much larger than contributions scaling as  $l_K$ .

Second, for long chains, our theory predicts little relaxation during deformation, and a strain hardening modulus  $G_R \simeq \rho l_0^2 l_K$ . This value is much closer to the effective constraint density measured in (NMR) experiments of deformed glassy samples [14] than to the entropic prediction  $G_R = \rho_e k_B T$ . Increasing  $l_K$  also increases  $\rho_e$  [53]; this makes relating hardening to entanglement a subtle problem. However,

considerable evidence (e.g., [9,19,23,36,37,54,55]) suggests that chain orientation and local secondary interactions which act over scales  $\sim(l_0 \sim a \sim l_K)$  are the true controlling factors for  $\sigma$  at least during the initial stages of hardening. Finally, Haward postulated that  $G_R$  arises from the constraints imposed by the mesh of uncrossable chains [11]; our argument that hardening scales with  $\rho_{cr}$  is consistent with this hypothesis.

### G. Predictions for stress-strain curves

In Eq. (15) we have assumed that all contributions to  $\sigma$  scale with a single energy density (i.e., stress)  $(u_0/a^3)$ . This is an approximation since flow and hardening stresses are typically linearly rather than directly proportional [56]. However, the “constant offset” term in this linear relationship is often fairly small compared to the linear term (especially for  $T$  well below  $T_g$  [23,56]), so the approximation is reasonable. Therefore, we associate  $u_0/a^3$  with  $\sigma_{flow}$  and scale it out. This gives

$$\sigma^*(\epsilon_{eff}) = A \frac{\sigma(\epsilon_{eff})}{u_0/a^3}, \quad (16)$$

where  $A$  is a prefactor arising from our neglect of prefactors in the above analysis. Note that all “thermal” aspects of our theory are implicitly wrapped into  $A$  and  $\tau_\alpha$ . In both real and simulated systems  $\sigma_{flow}$  and  $A$  are approximately proportional to  $(1-T/T_g)$  [12,20,42,57], so this scaling should remove much of the  $T$  dependence. The merits of “multiplicative” forms like Eq. (16) for predicting stress have been discussed recently in Refs. [37,58]. More sophisticated models (e.g., Ref. [9]) explicitly treat the variation of  $A$  with  $\epsilon$  and  $T$  and/or the variation of  $\tau_\alpha$  with  $\sigma$ ,  $T$ , and local microstructure. Here, however,  $A$  and (for fixed  $N$ )  $\tau_\alpha$  are treated as numerical constants [59].

To predict the  $N$  dependence of  $\sigma(\epsilon)$ , an analytic form for  $g[\epsilon_{eff}(\epsilon)]$  is obtained by plugging the solution for  $\epsilon_{eff}(\epsilon)$  from Eq. (7) into the form of  $g(\epsilon)$  for uniaxial deformation [Table I, with  $\exp(\epsilon)=\lambda$ ],

$$g(\epsilon_{eff}(\epsilon)) = \exp\{2\dot{\epsilon}\tau[1 - \exp(-\epsilon/\dot{\epsilon}\tau)]\} - \exp[-\dot{\epsilon}\tau[1 - \exp(-\epsilon/\dot{\epsilon}\tau)]]. \quad (17)$$

Figure 4 shows predictions of Eqs. (16) and (17) for  $\sigma^*(\epsilon)$  in uniaxial compression at various  $N$ , with  $A=1$ ,  $|\epsilon_y|=0.02$ ,  $\rho=1.0a^{-3}$ ,  $l_0=0.96a$ , and  $l_K=1.8a$ ; the latter three are chosen to match the flexible bead-spring model employed in the simulations. Solid lines assume  $\tau \propto N^{\gamma-1}$  with  $\gamma=2$  as discussed above, while symbols assume that coherent chain relaxation is not important and  $\tau \propto N^\gamma$ . The solid lines are qualitatively consistent with simulations [22,57], while the symbols are inconsistent. Both show increasing strain hardening with increasing  $N$ , but in the latter case hardening increases much faster and saturates at a much lower value of  $N$  than is realistic. For example, the  $\tau \propto N^\gamma$  predictions for  $N=40$  and  $N=500$  are indistinguishable on the scale of the plot. Results for tension are not presented here because our model includes no asymmetry between tension and compression [60].

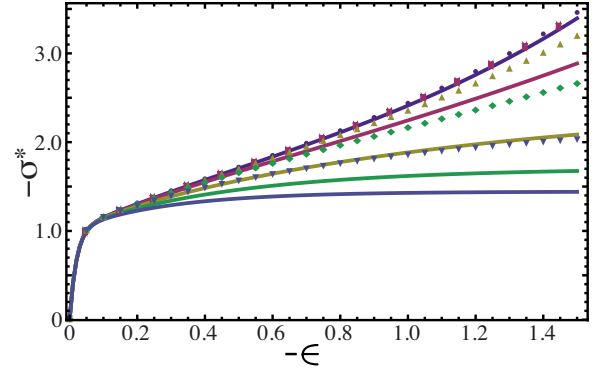


FIG. 4. (Color online) Stress-strain curves predicted in Eqs. (16) and (17) with  $A=1$ .  $-\sigma^*$  and  $-\epsilon$  are shown because stress and strain are negative for compression. Curves from top to bottom are for  $N=500$ ,  $N=10$ ,  $N=5$ , and  $N=3$ . Predictions in the  $N \rightarrow \infty$  limit are not distinguishable from  $N=500$  predictions on the scale of this plot. Solid curves assume  $\dot{\epsilon}\tau = BN^{\gamma-1}$ , while symbols assume  $\dot{\epsilon}\tau = BN^\gamma$ . In both cases,  $\gamma=2$ , and as suggested in Ref. [8]  $B=0.1$ .

The large-strain ( $\epsilon \gg \epsilon_y$ ) mechanical response predicted by our model varies continuously from perfect-plastic flow [ $\sigma^*(\epsilon) \rightarrow$  a constant  $\sigma_{flow}$ ] to networklike polymeric response [ $\sigma^*(\epsilon) \rightarrow 1 + \rho l_0^2 l_K g(\epsilon)/2$ ] as  $\dot{\epsilon}\tau$  varies from zero to  $\infty$  (equivalently, as  $N$  increases). In between these limits, the response is “polymeric viscoplasticity” (or more accurately “viscoelastoplasticity” since we treat  $\epsilon_{eff}$  as microreversible [61]). However, since our model does not treat stress relaxation after cessation of deformation,  $\sigma^*$  may be regarded as a (reduced) orientation-dependent plastic flow stress.

We now compare theoretical predictions for stress-strain curves to results from bead-spring simulations. In Fig. 5, dashed lines show predictions of Eqs. (16) and (17) with  $A=0.43$ , values of  $\tau$  taken from Table II, and the same values of  $|\epsilon_y|$ ,  $l_0$ , and  $l_K$  as in Fig. 4. The value of  $A$  obtained in Fig. 5 is comparable to  $(1-T/T_g)$ . Stress-strain curves from simulations are shown as solid lines. Panel (a) shows  $\sigma^*$ , while panel (b) shows its dissipative component  $\sigma^{Q*} = [\sigma^* - (u_0/a^3)^{-1} \partial U / \partial \epsilon]$  [22]. While this definition of  $\sigma^{Q*}$  includes entropic terms, these are very small, on the order of 1% of the total stress at this  $T$  [22].

In both panels, the correct trends are predicted, and quantitative agreement is within  $\sim 20\%$ . Very short chains ( $N=4$ ) show nearly perfect-plastic flow, while longer chains show strain hardening similar to results analyzed in many previous studies. The quantitative differences at small strains arise primarily from our oversimplified treatment of yield [62]. At large strains, comparing panels (a) and (b), it is apparent that differences between predictions of Eqs. (16) and (17) and simulation results arise largely from energetic terms associated with strain hardening, i.e., covalent bond energy and additional plastic deformation arising from chain stretching between entanglements. Experiments on amorphous polymer glasses (e.g., [19]) have shown that a similar percentage of the total stress is associated with energetic terms, strain softening, etc., so the agreement between theoretical predictions and bead-spring results is satisfactory given the simplicity of our model. In panel (b), the “spike” in simulation results at small strains for  $N > 4$  reflects yield and subsequent strain softening.

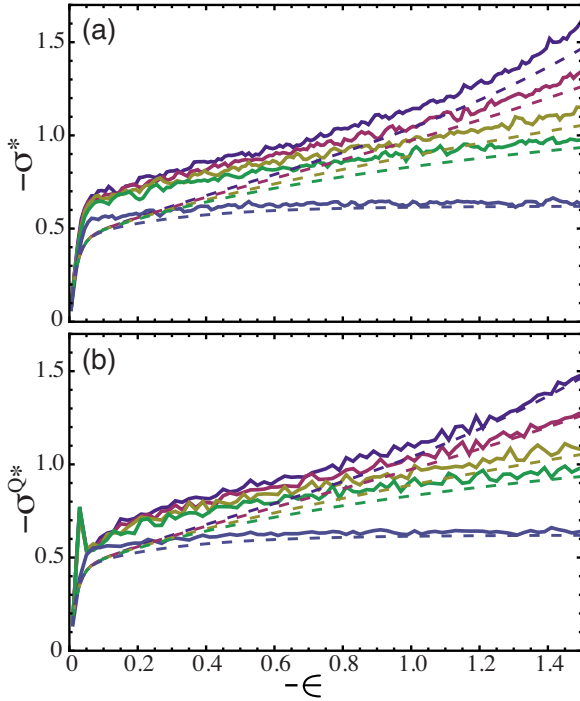


FIG. 5. (Color online) Stress-strain curves [(a)  $\sigma^*$ ; (b)  $\sigma^{Q*}$ ] from bead-spring simulations (solid lines) and theoretical predictions (dashed lines) in Eqs. (16) and (17). Values of  $N$  from top to bottom are 500, 36, 18, 12, and 4. The top 4 are from the same simulations shown in Fig. 3 and use the fit values of  $\tau$  (Table II), while the bottom theory curve assumes  $\dot{\epsilon}\tau=0.1(N-1)$ . Note that stresses and strains are negative in compression.

### H. Nonaffine displacement and plastic deformation

We have argued above that coherent relaxation is driven by the stiff covalent bonds and the need to maintain constant chain contour length  $L$ . Since long chains have  $\dot{\epsilon}\tau \gg 1$  and deform affinely on the end-to-end scale, they must deform nonaffinely on smaller scales to maintain chain connectivity. It is interesting to relate this nonaffine deformation to the chain stretching that would occur if deformation was affine on all scales and  $L$  was not constrained, i.e., the limit of a Gaussian coil with zero spring constant [2] embedded in a deforming medium. For uniaxial tension or compression the nonaffine displacement should be given by  $D_{na}^2 \sim S(\lambda)-1$ , with

$$S(\lambda) \equiv \frac{L(\lambda)}{L(1)} = \frac{1}{2} \left( \lambda + \frac{\sin^{-1}(\sqrt{1-\lambda^3})}{\sqrt{\lambda-\lambda^4}} \right). \quad (18)$$

Figure 6 shows data for the squared nonaffine displacement of monomers,  $D_{na}^2 = \langle (\vec{r} - \bar{\lambda}\vec{r}_0)^2 \rangle$ , where the monomer positions are  $\{\vec{r}\}$  at stretch  $\bar{\lambda}$  and  $\{\vec{r}_0\}$  in the initial state, for  $N=500$ . Data for  $T=0.01u_0/k_B$  are shown to minimize the thermal contribution to  $D_{na}^2$ . A fit to  $S(\lambda)-1$  is also displayed. There is qualitative agreement at large strains ( $\lambda \ll 1$ ), and the underestimation of  $D_{na}^2$  at smaller strains is largely attributable to smaller scale (i.e., incoherent) plasticity on scales approaching the monomer diameter  $a$ . Another reasonable form for fitting to  $D_{na}^2$  is  $\bar{g}(\lambda)$ , which would suggest  $D_{na}^2$

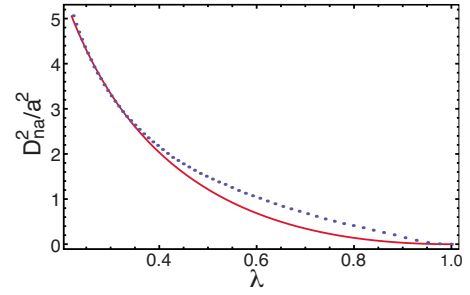


FIG. 6. (Color online) Nonaffine displacement at low  $T$  in systems of long chains. Circles show data from bead-spring simulations (with  $N=500$  and  $T=0.01u_0/k_B$ ). The solid line shows a fit to  $D_{na}^2/a^2 = C[S(\lambda)-1]$  [see Eq. (18)] with  $C=7.39$ . Note that the maximum value of  $D_{na}^2$  is well below the squared tube diameter  $d_T^2/a^2 \sim 100$  [2,46], consistent with the picture that entanglements do not control the mechanical response of these systems.

scales with  $W^p$  at large strains. This form gives slightly less good fits to our data, but in any case the principle shown in Fig. 6 is the same as outlined in Ref. [63]; for long chains, nearly affine deformation at large scales (in our language,  $\lambda \approx \lambda_{eff}$ ) increasingly drives nonaffine displacements (i.e., plastic activity) at smaller scales, leading to strain hardening. This effect weakens and values for both  $\sigma$  and  $D_{na}^2$  decrease (for large strains) with decreasing  $N$ .

### III. DISCUSSION AND CONCLUSIONS

We derived a simple theory for polymeric strain hardening based on the notion that the increase in stress beyond yield amounts to an increase in the “flow” stress in an increasingly anisotropic viscoplastic medium. In the strain hardening regime, long and short chains relax on large scales via similar mechanisms ( $\tau \propto \dot{\epsilon}^{-1}N$ ) and longer chains show greater hardening because they cannot relax on large length scales over the time scale of the deformation. In practice, this is due to the high interchain friction in the glassy state.

We theoretically predicted and provided evidence using simulations that coherent chain relaxation driven by resistance to chain contour length increase is a key factor in the large-strain mechanical response of uncross-linked polymer glasses. Coherent relaxation reduces the dominant (chain scale) relaxation time  $\tau$  by a factor  $N\dot{\epsilon}$  during active deformation. Further, we claim that the increase in relaxation times when deformation is ceased is at least partially associated with the fact that relaxation need no longer be coherent. Our results are consistent with many previous simulations and experiments and semiquantitatively capture the increase in strain hardening as chain length increases.

Much recent work has emphasized the predominantly viscous or viscoelastic nature of polymeric strain hardening, at least prior to entanglement stretching. Recent experiments and modeling [37,54,58,64] have provided strong support to the notion that entanglements play only a secondary role in glassy-polymeric strain hardening, at least for the majority of synthetic polymers and in the weak hardening regime. Hine and co-workers [54,64] also emphasized the role of meltlike relaxation mechanisms in the marginally glassy state.

The present work, which focuses on relaxation mechanisms, is consistent with these trends. We quantitatively related strain hardening to local plasticity at the segmental scale and showed that the power-law dependence of the large-scale chain relaxation time  $\tau$  on  $N$  during active deformation,  $\tau \propto N^{\gamma-1}$ , is consistent with  $\gamma=2$ , the same value as the Rouse model for unentangled polymer melts [2,65,66]. Another “Rouselike” aspect is the apparent tight coupling of  $\tau$  to a single microscopic relaxation time  $\tau_\alpha$ .

$\lambda_{eff}$  can now be accurately measured in scanning near-field optical microscopy (SNOFM) experiments [67], which have shown that  $\epsilon_{eff} < \epsilon$  for entangled chains deformed slightly above  $T_g$ . Analogous studies, well below  $T_g$ , could be performed to test the theory developed here; modern neutron-scattering techniques might be employed for the same purpose. Additionally, deformation calorimetry (DC) experiments [68] can be performed to better understand the dissipative contribution to the stress. We are not aware of any studies in which the SNOFM or DC methods have been applied to study strain hardening in polymer glasses.

Our model is minimal. It cannot quantitatively predict stress-strain curves either at small or at very large strains because it neglects energetic components of stress and also strain softening, which play important roles in glassy polymer mechanics. However, these limitations do not violate the spirit of our modeling effort, which was to illustrate the role of coherent relaxation in controlling large-scale chain conformations and influencing stress in actively deforming polymer glasses.

The theory presented here serves as a complement to a recent microscopic theory by Chen and Schweizer [9], which also provides a unified description of plastic flow and strain hardening in polymer glasses. However, Ref. [9] assumes  $\bar{\lambda}_{eff} = \bar{\lambda}$ , is based on an extension of liquid state theory to the glassy state [8], and (formally) breaks down at  $T=0$ . In contrast, the theory developed here assumes that relaxation is dominated by strain-activated processes and so should be

most accurate at low temperatures. We expect it to break down concurrently with the validity of the mean-field independent-chain-relaxation behavior [23] of  $\lambda_{eff}$  as  $T \rightarrow T_g$ .

An ideal approach would explicitly account for both thermally and strain-activated relaxation without sacrificing simplicity. For example, stress-assisted rearrangements should reduce  $\tau$  as  $|\sigma|$  increases, and thermal activation should produce logarithmic corrections to  $\epsilon^{-1}$  scaling. Combining our theory for large-scale chain relaxation with a more sophisticated theory for  $\sigma_{flow}$  (e.g., Refs. [8] or [48]) might be fruitful. Modern techniques in the nonequilibrium thermodynamics of internal state variables [13,28] may also prove useful in this effort.

Clearly, further work is necessary to quantitatively predict stress-strain and stress-relaxation curves. In particular, improved understanding of the effects of chain stiffness is required. It seems certain that microscopic structural detail at the Kuhn scale (e.g., chemistry-dependent effects) exerts significant influence on segmental relaxation processes, and it is probable that these effects couple to chain-scale relaxation (see, e.g., Refs. [6,13,40,56,63,67,68]). Studies using more chemically realistic models or real polymers would be welcome.

#### ACKNOWLEDGMENTS

Mark O. Robbins contributed significantly to this project, with numerous helpful discussions. Kenneth S. Schweizer, Grigori Medvedev, Kang Chen, Daniel J. Read, Robert A. Riggleman, and Edward J. Kramer also provided helpful discussions and K. S. provided the original concept for  $\lambda_{eff}$ . Gary S. Grest provided equilibrated  $N=500$  states. The authors are grateful to the organizers of the KITP Glasses '10 conference. Support from NSF Awards No. DMR-0520415 (R.S.H.) and No. DMR-0835742 (R.S.H. and C.S.O.) is gratefully acknowledged.

- 
- [1] *The Physics of Glassy Polymers*, 2nd ed., edited by R. N. Haward and R. J. Young (Chapman and Hall, London, 1997).
  - [2] M. Doi and S. F. Edwards, *The Theory of Polymer Dynamics* (Clarendon Press, Oxford, 1986).
  - [3] L. S. Loo, R. E. Cohen, and K. K. Gleason, *Science* **288**, 116 (2000).
  - [4] H. N. Lee, R. A. Riggleman, J. J. de Pablo, and M. D. Ediger, *Macromolecules* **42**, 4328 (2009).
  - [5] H. N. Lee, K. Paeng, S. F. Swallen, and M. D. Ediger, *Science* **323**, 231 (2009).
  - [6] F. M. Capaldi, M. C. Boyce, and G. C. Rutledge, *Phys. Rev. Lett.* **89**, 175505 (2002); *Polymer* **45**, 1391 (2004).
  - [7] R. A. Riggleman, K. S. Schweizer, and J. J. de Pablo, *Macromolecules* **41**, 4969 (2008); R. A. Riggleman, H.-N. Lee, M. D. Ediger, and J.-J. de Pablo, *Soft Matter* **6**, 287 (2010).
  - [8] K. Chen and K. S. Schweizer, *EPL* **79**, 26006 (2007); *Macromolecules* **41**, 5908 (2008); K. Chen, E. J. Saltzman, and K. S. Schweizer, *J. Phys.: Condens. Matter* **21**, 503101 (2009).
  - [9] K. Chen and K. S. Schweizer, *Phys. Rev. Lett.* **102**, 038301 (2009).
  - [10] L. Grassia and A. D'Amore, *J. Polym. Sci., Part B: Polym. Phys.* **47**, 724 (2009).
  - [11] R. N. Haward, *Macromolecules* **26**, 5860 (1993).
  - [12] A. S. Argon, *Philos. Mag.* **28**, 839 (1973).
  - [13] J. Hintermeyer, A. Herrmann, R. Kahlau, C. Goiceanu, and E. A. Rössler, *Macromolecules* **41**, 9335 (2008).
  - [14] M. Wendlandt, T. A. Tervoort, J. D. van Beek, and U. W. Suter, *J. Mech. Phys. Solids* **54**, 589 (2006).
  - [15] L. R. G. Treloar, *The Physics of Rubber Elasticity* (Clarendon Press, Oxford, 1975).
  - [16] A more accurate form for this increase which accounts for non-Gaussian effects predicts  $\sigma \sim g^* = \ell^{-1}[\bar{g}(\bar{\lambda}/\sqrt{N_e})]g(\lambda)$ , where  $\ell$  is the Langevin function.
  - [17] E. M. Arruda and M. C. Boyce, *Int. J. Plast.* **9**, 697 (1993); *J. Mech. Phys. Solids* **41**, 389 (1993).
  - [18] E. J. Kramer, *J. Polym. Sci., Part B: Polym. Phys.* **43**, 3369

- (2005).
- [19] O. A. Hasan and M. C. Boyce, *Polymer* **34**, 5085 (1993).
- [20] H. G. H. van Melick, L. E. Govaert, and H. E. H. Meijer, *Polymer* **44**, 2493 (2003).
- [21] M. Dettenmaier, A. Maconnachie, J. S. Higgins, H. H. Kaush, and T. Q. Nguyen, *Macromolecules* **19**, 773 (1986).
- [22] R. S. Hoy and M. O. Robbins, *Phys. Rev. Lett.* **99**, 117801 (2007); *Phys. Rev. E* **77**, 031801 (2008).
- [23] R. S. Hoy and M. O. Robbins, *J. Chem. Phys.* **131**, 244901 (2009).
- [24] Very short chains do not significantly orient, and (if brittle fracture does not intervene) oligomeric glasses show nearly perfect-plastic flow, similar to that observed in atomic glasses [22,57]; Eq. (1) still applies in this case because  $\bar{\lambda}_{eff} \approx \bar{l}$  and  $g(\bar{l})=0$ .
- [25] L. Anand and M. E. Gurtin, *Int. J. Solids Struct.* **40**, 1465 (2003); J. M. Caruthers, D. B. Adolf, R. S. Chambers, and P. Shrikhande, *Polymer* **45**, 4577 (2004); R. B. Dupaix and M. C. Boyce, *Mech. Mater.* **39**, 39 (2007).
- [26] M. Wendlandt, T. A. Tervoort, and U. W. Suter, *Polymer* **46**, 11786 (2005).
- [27] Our theory can be viewed as a mesoscopic counterpart of the pseudoaffine model of Brown *et al.* [29], which relates  $\lambda$  to *microscopic* orientation at the Kuhn segment level. Previous theoretical treatments of  $\lambda \neq \lambda_{eff}$  (e.g., Refs. [30,31]) have been phenomenological and included many adjustable parameters. Cheng *et al.* [30] noted that a Maxwell-model formulation for  $\lambda \neq \lambda_{eff}$  (employed therein) is mathematically equivalent to transient network elasticity, which predicts [32] a  $g(\epsilon)$  similar to Eq. (17).
- [28] M. B. Rubin, *Int. J. Solids Struct.* **31**, 2635 (1994).
- [29] D. J. Brown and A. H. Windle, *J. Mater. Sci.* **19**, 1997 (1984); G. R. Mitchell, D. J. Brown, and A. H. Windle, *Polymer* **26**, 1755 (1985).
- [30] H. L. Cheng, J. Wang, and Z. P. Huang, *Mech. Time-Depend. Mater.* **14**, 261 (2010).
- [31] C. Miehe, S. Göktepe, and J. Méndez Diez, *Int. J. Solids Struct.* **46**, 181 (2009).
- [32] M. S. Green and A. V. Tobolsky, *J. Chem. Phys.* **14**, 80 (1946).
- [33] Restoration of  $\epsilon_{eff}$  toward its equilibrium value (zero) can, in principle, drive shape recovery in a stress-relaxation experiment; motions decreasing  $|\epsilon_{eff}|$  correspond roughly to the “reverse shear transformations” [12] studied by many authors. However, treatment of such effects is beyond the scope of this work. In practice, the time scale of relaxation of  $|\epsilon_{eff}|$  after a large deformation would be very long if  $T$  is well below  $T_g$ .
- [34] B. Gross and R. M. Fuoss, *J. Polym. Sci.* **19**, 39 (1956).
- [35] In practice, systems are “densely” entangled if  $N_e l_0 \lesssim 10 l_K$  [22].
- [36] T. Ge and M. O. Robbins, *J. Polym. Sci., Part B: Polym. Phys.* **48**, 1473 (2010).
- [37] D. J. A. Senden, J. A. W. van Dommelen, and L. E. Govaert, *J. Polym. Sci., Part B: Polym. Phys.* **48**, 1483 (2010).
- [38] K. Kremer and G. S. Grest, *J. Chem. Phys.* **92**, 5057 (1990).
- [39] S. Plimpton, *J. Comput. Phys.* **117**, 1 (1995).
- [40] A. V. Lyulin and M. A. J. Michaels, *J. Non-Cryst. Solids* **352**, 5008 (2006).
- [41] R. Auhl, R. Everaers, G. S. Grest, K. Kremer, and S. J. Plimpton, *J. Chem. Phys.* **119**, 12718 (2003).
- [42] J. Rottler and M. O. Robbins, *Phys. Rev. E* **68**, 011507 (2003).
- [43] M. O. Robbins and R. S. Hoy, *J. Polym. Sci., Part B: Polym. Phys.* **47**, 1406 (2009).
- [44] Eq. (7) predicts “saturation” of orientation and hardening at large strains  $\epsilon_{eff} \gtrsim \epsilon_{eff}^{sat} = \dot{\epsilon} \tau$ . (It can be rewritten as  $\epsilon_{eff}(\epsilon) = \epsilon_{eff}^{sat} [1 - \exp(-\epsilon / \epsilon_{eff}^{sat})]$ .) Our theory will break down in the limit where chains are pulled taut, i.e.,  $\tilde{g}(\epsilon_{eff}^{sat}) \sim N l_0 / l_K$ . However, this limit is difficult to reach at experimentally accessible strains.
- [45] R. S. Hoy, K. Foteinopoulou, and M. Kröger, *Phys. Rev. E* **80**, 031803 (2009).
- [46] R. Everaers, S. K. Sukumaran, G. S. Grest, C. Svaneborg, A. Sivasubramanian, and K. Kremer, *Science* **303**, 823 (2004); J.-X. Hou, C. Svaneborg, R. Everaers, and G. S. Grest, *Phys. Rev. Lett.* **105**, 068301 (2010).
- [47] M. Warren and J. Rottler, *Phys. Rev. Lett.* **104**, 205501 (2010).
- [48] M. C. Boyce, D. M. Parks, and A. S. Argon, *Mech. Mater.* **7**, 15 (1988).
- [49] C. Chui and M. C. Boyce, *Macromolecules* **32**, 3795 (1999); J. Li, T. Mulder, B. Vorselaars, A. V. Lyulin, and M. A. J. Michels, *ibid.* **39**, 7774 (2006).
- [50] In Sec. II F,  $u_0$  and  $a$  are intended to be interpreted generally; they need not necessarily correspond to the interaction potentials employed in our simulations.
- [51] Other recent work [26,37,58] relates the rate dependence and nonlinearity of strain hardening to an Eyring-like model in which the activation volume  $V$  decreases with increasing strain. In contrast, we predict that  $V$  increases. An important difference between the approaches is that in the Eyring-like models,  $V$  is a parameter with the dimensions of volume rather than a physical volume.
- [52] Similar ambiguities arise in theoretical prediction of the melt plateau modulus  $G_N^0$  from chain microstructure: W. W. Graessley and S. F. Edwards, *Polymer* **22**, 1329 (1981).
- [53] L. J. Fetters, D. J. Lohse, S. T. Milner, and W. W. Graessley, *Macromolecules* **32**, 6847 (1999).
- [54] P. J. Hine, A. Duckett, and D. J. Read, *Macromolecules* **40**, 2782 (2007).
- [55] Fitting experimental curves to  $G_R = \rho_e k_B T$  produces values of  $\rho_e$  about 100 times larger (near  $T_g$ ) [18,20,57] than values measured in melt-rheological experiments.
- [56] L. E. Govaert, T. A. P. Engels, M. Wendlandt, T. A. Tervoort, and U. W. Suter, *J. Polym. Sci., Part B: Polym. Phys.* **46**, 2475 (2008).
- [57] R. S. Hoy and M. O. Robbins, *J. Polym. Sci., Part B: Polym. Phys.* **44**, 3487 (2006).
- [58] M. Wendlandt, T. A. Tervoort, and U. W. Suter, *J. Polym. Sci., Part B: Polym. Phys.* **48**, 1464 (2010).
- [59] R. B. Dupaix and M. C. Boyce, *Polymer* **46**, 4827 (2005).
- [60] This asymmetry has been treated in other work (see, e.g., Refs. [42,48]) and could, in principle, be treated by modifying  $W^s$  appropriately.
- [61] Senden *et al.* [37] also treated glassy polymers as Neo-Hookean viscoelastoplastics using a continuum model with a phenomenological mixing of reversible and irreversible contributions to the stress.
- [62] Interestingly, our theoretical stress-strain curves are remarkably similar to those in preoriented systems where deformation is applied along the preorientation direction: see, e.g., Fig. 1(b) of Ref. [36] and Fig. 3(b) of Ref. [37].

- [63] B. Vorselaars, A. V. Lyulin, and M. A. J. Michels, *Macromolecules* **42**, 5829 (2009).
- [64] D. S. A. de Focatiis, J. Embery, and C. P. Buckley, *J. Polym. Sci., Part B: Polym. Phys.* **48**, 1449 (2010); K. Nayak, D. Read, T. C. B. McLeish, P. Hine, and M. Tassieri, *J. Polym. Sci., Part B: Polym. Phys.* (to be published).
- [65] Our results do not exclude the possibility of a crossover to higher  $\gamma$  for chains with  $N \gg N_e$ . Govaert and Tervoort [65] presented data for  $N \gg N_e$  systems that suggest hardening and melt relaxation vary similarly with  $N$  (i.e., both are dominated by large-scale relaxation). Although data were interpreted in terms of relaxation of the entanglement network, the results are not inconsistent with ours because  $\gamma$  was not measured. Few other experimental studies have systematically examined the variation of large-strain glassy response with  $N$ , but recent data for quiescent dynamics near  $T_g$  [13] suggest that the presence of absence of any large- $N$  crossover in  $\gamma$  may be chemistry dependent.
- [66] L. E. Govaert and T. A. Tervoort, *J. Polym. Sci., Part B: Polym. Phys.* **42**, 2041 (2004).
- [67] T. Ube, H. Aoki, S. Ito, J. Horinaka, and T. Takigawa, *Polymer* **48**, 6221 (2007); T. Ube, H. Aoki, S. Ito, J. Horinaka, T. Takigawa, and T. Masuda, *ibid.* **50**, 3016 (2009).
- [68] G. W. Adams and R. J. Ferris, *J. Polym. Sci., Part B: Polym. Phys.* **26**, 433 (1988).